MAUSAM, **77**, 3 (July 2026),1093-1100

MAUSAM

DOI: https://doi.org/10.54302/mausam.v77i3.6622
Homepage: https://mausamjournal.imd.gov.in/index.php/MAUSAM

UDC No.551.577.22:551.576.3:528.88

Passive microwave remote sensing of soil moisture for flood prediction: A case study of Derna, Libya

*BIKRAMJIT GOSWAMI and MANORANJAN KALITA

Assam Don Bosco University, Azara, Guwahati, India- 781017

(*Received 19 April 2024, Accepted 1 December 2025*)

***Corresponding author's email: bikramjit.goswami@dbuniversity.ac.in**

सार – बाढ़ के शुरुआती संकेतों की पहचान करने में मिट्टी की नमी और वर्षण जैसे पर्यावरणीय कारकों की निरंतर निगरानी एक महत्वपूर्ण भूमिका निभाती है, विशेष रूप से चरम मौसम के प्रति संवेदनशील क्षेत्रों में। पैसिव माइक्रोवेव रिमोट सेंसिंग इस संदर्भ में अपनी नियमित दैनिक कवरेज के साथ, मौसम की स्थिति की परवाह किए बिना डेटा एकत्र करने की क्षमता के कारण विशिष्ट है। इस अध्ययन में, 11 सितंबर 2023 को डर्ना, लीबिया में आई भीषण बाढ़ से पहले और बाद में ध्रुवीकरण सूचकांक (Polarisation Index - PI) में बदलाव की जांच की गई थी। उपयोग किया गया डेटा जापान के GCOM-W1 सैटेलाइट पर सवार X-बैंड (10 GHz) पर काम करने वाले AMSR2 सेंसर से प्राप्त किया गया था। विशेष रूप से, बाढ़ से एक दिन पहले PI में भारी वृद्धि दर्ज की गई थी, जो क्षेत्र में तीव्र वर्षा से जुड़ी मिट्टी की नमी में वृद्धि के अनुरूप थी। घटना के बाद, PI मान ऊंचे बने रहे, जो निरंतर भूमि संतृप्ति (Ground saturation) का संकेत देते हैं। ये निष्कर्ष भारी वर्षा और बाढ़ के जोखिम के लिए एक प्रारंभिक चेतावनी संकेतक के रूप में PI की क्षमता की ओर इशारा करते हैं। अवलोकन बिंदुओं के उचित चयन के साथ, यह विधि दुनिया भर के अन्य उच्च जोखिम वाले क्षेत्रों में बाढ़ पूर्वानुमान प्रणालियों के विकास का समर्थन कर सकती है।

ABSTRACT. Monitoring environmental factors such as soil moisture and precipitation on a frequent basis plays a vital role in identifying early signs of flooding, particularly in regions prone to extreme weather. Passive microwave remote sensing stands out in this context due to its ability to collect data regardless of weather conditions, along with its regular daily coverage. In this study, changes in the Polarisation Index (PI) were examined before and after the severe flooding that struck Derna, Libya, on 11 September 2023. The data used were obtained from the AMSR2 sensor operating at X-band (10 GHz) aboard Japan's GCOM-W1 satellite. Notably, a sharp rise in PI was recorded one day ahead of the flood, aligning with increased soil moisture linked to intense rainfall in the area. Following the event, PI values remained elevated, indicating continued ground saturation. These findings point to the potential of PI as an early warning indicator for heavy rainfall and flood risk. With appropriate selection of observation points, this method could support the development of flood forecasting systems in other high-risk regions around the world.

Key words – Remote Sensing, Brightness Temperature, Polarization Index, Flood, Precipitation..

1. Introduction

Microwave radiometry is a widely used remote sensing method in geoscientific research. Microwave remote sensing is especially useful in the regions experiencing extensive cloud cover during the monsoon season (Ulaby, 1976). Moreover, operational meteorology and oceanography are benefiting significantly from the use of microwave sensors on earth-orbiting satellites, as indicated in several literatures (Njoku, 1982). Initially airborne and spaceborne sensors were used in microwave remote sensing studies, carried out during the 1970's and 80's. These sensors are currently being developed into operational satellite observation systems, having faster and advanced earth observing capabilities (Hariharan and Pandey, 1983). A significant portion of the Earth's land area may be sampled daily for change monitoring and soil moisture measurement, using microwave readings taken from the high-altitude satellites (Njoku and Entekhabi, 1996).

Microwaves' capacity to penetrate through the objects allows for a variety of applications, including the monitoring and operation during the cloudy, rainy and foggy days (Peichl, *et al*., 2007). The heat radiation from the viewed surfaces during all weather conditions is measured by very sensitive, reliable passive microwave receivers (Pampaloni, 2014). Thus, microwave radiometry is a measuring method based on target materials with the microwave emission from the thermal content of the body (Peichl, et al., 2015). This characteristic emission of the target material helps in detecting changes in the remote sensing applications.

The Special Sensor Microwave/Imager (SSM/I) and the Special Sensor Water Vapor Sounder (SSM/T2) onboard the polar orbiting Defence Meteorological Satellite Program (DMSP), and the Advanced Microwave Scanning Radiometer 2 (AMSR2) sensor, which was launched on the Global Change Observation Mission 1st-Water, "SHIZUKU" (GCOM-W1) satellite by the Japan Aerospace Exploration Agency (JAXA), are examples of some of the operating polar orbiting platforms with passive microwave sensors. Passive microwave sensors on such satellites usually operate between 6 and 183 GHz, offering useful data on the distributions of water vapor, liquid water, ice, and rainfall, as well as other atmospheric components of the hydrological cycle. Both short-term/regional applications for observing severe weather and long-term/global applications for monitoring the climate change and validating climate models show the great utility of microwave measurements (Bauer, 1995).

For regional-scale flooding events that take place over time periods of days to weeks, predictability is a critical factor. Remote sensing measurements improve such estimates of the timing and severity of the flood peak. The potential of remotely sensed soil moisture in flood forecasting applications is demonstrated very well using data from the Advanced Microwave Sensing Radiometer (AMSR-E). Low brightness temperatures, or the maximum soil moisture levels, across the afflicted areas prior to the peak streamflow conditions, are a strong indication of an impending disaster (Bindlish, et al., 2004).

2. Data and methodology

2.1. *Flood in Derna, Libya*

The Eastern Libyan port city Derna is situated between the Mediterranean Sea, the desert, and Jebel Akhdar Mountain, popularly known as Green Mountain. Therefore, Derna has a special geographical setting compared to other cities in Libya. Derna is situated near the eastern extremity of the Jebel Akhdar, one of the country's few forested regions, hence experiences an arid climate. Forests only cover 0.1% of Libya's total land area. However, the lush upland region of eastern Libya, which receives about 600 millimetres (24 in) of precipitation annually, is close to Derna. The city is situated alongside the ephemeral Wadi Derna River. Floods have historically repeatedly caused harm to the city (Marshall, 2023).

It is reported that the devastating floods which struck Derna and surrounding areas in Libya on 11 September 2023 have claimed as many as 20,000 lives. The collapse of two dams, unable to withstand the intense pressure from accumulated water, released an estimated 30 million cubic metres into the city. Several nearby towns were also severely affected. The floods were triggered by extreme rainfall — more than an entire year's precipitation falling within a single day. According to the World Meteorological Organization (WMO), based in Geneva, several parts of Libya received between 150 and 240 millimetres of rainfall during the storm. In the village of Al-Bayda, record 414.1 millimetres rainfall happened within just 24 hours. Usually, Derna typically receives around 274 millimetres of rain over the course of an entire year, as reported by the German Weather Service (Abu-Aziza, *et al.*, 2017).

Flooding experts note the extremely heavy rainfall, which was likely made worse by supercharging Storm Daniel. This storm had developed over the Mediterranean Sea around 4th September 2023 due to a low-pressure weather system. This storm, according to the WMO, resulted into a record-breaking rainfall in Greece on September 5 and 6. The storm then became a Medicane, a Mediterranean storm, with hurricane-like features, as it grew stronger over the water. It touched down in Libya on September 10, 2023.

The Al-Bilad and Abu Mansur dams upstream of Derna city were meant to control soil erosion and prevent flooding. However, on 10 September, intense rainfall led to a rapid build-up of water flowing down from the nearby mountains, which ultimately caused both dams to collapse under the pressure. The deaths and flood-related damage in Derna appear to be strongly influenced by these dam-breaks, which could not be predicted in advance by any existing monitoring system (Meteoblue, 2024).

Table 1 shows the coordinates of some of the above-mentioned locations, which are studied using AMSR2 passive microwave remote sensing images of spatial resolution 10 km × 10 km, as described in the subsequent sections.

Recent studies over the past few years have emphasized the critical role of passive microwave remote sensing in flood monitoring and soil moisture estimation, particularly under all-weather conditions and frequent revisit times. Research highlights the effectiveness of satellite-based root zone soil moisture measurements

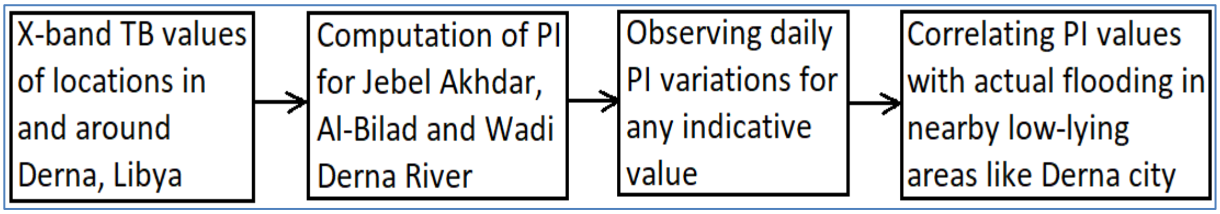

Fig. 1. The methodology used for studying the PI variations for areas near Derna, Libya

TABLE 1

Locations considered for studying the Passive Microwave Remote Sensed features

Location	Point name used for PI computation	Latitude (ºN)	Longitude (ºE)
Derna City	Derna City	32.7	22.6
Jebel Akhdar Mountain Region Location 1	Al-Bilad1	32.6	22.5
Al-Bilad Dam	Al-Bilad2	32.6	22.6
Jebel Akhdar Mountain Region Location 2	Al-Bilad3	32.5	22.5
Wadi Derna River Course Location 1	Al-Bilad4	32.5	22.6
Jebel Akhdar Mountain Region Location 3	Al-Bilad5	32.4	22.5
Wadi Derna River Course Location 2	Al-Bilad6	32.4	22.6

using passive microwave sensors, which provide vital continuous data for early flood detection (Kasim, *et al.*, 2025). Researchers also demonstrated that passive microwave observations surpass optical and SAR sensors during extreme weather by consistently monitoring surface water and soil moisture anomalies indicative of flood risks (Febrian, *et al.*, 2025). Integrating these remote sensing data with machine learning enhances flood susceptibility mapping and prediction accuracy (Hajji, *et al.*, 2025). Further works confirmed that passive microwave indices reliably correlate with river discharge and can detect flood magnitude, especially in data-sparse regions (Mokkenstorm, *et al.*, 2021).

The recent advances focus on the promise of polarization-based indices, such as the Polarisation Index (PI), to detect pre-flood soil saturation and heavy rainfall conditions, as applied in the Derna, Libya flood event. These studies collectively demonstrate that passive microwave remote sensing, combined with targeted indices, offers a powerful toolset for real-time flood forecasting and disaster preparedness.

2.2. *Methodology*

The methodology used for detecting the major variations of passive microwave remote sensed features is illustrated in fig. 1. The X-band brightness temperature (TB) values are extracted from the passive microwave remote sensed images of Advanced Microwave Scanning Radiometer 2 (AMSR-2) sensor on board GCOM-W1 satellite.

The polarization index (*PI*) values are then computed from the TB values of the corresponding locations near Derna city. The mathematical technique used for computation of PI for eliminating the effect of surface temperature component of TB is briefly illustrated in the following.

$$PI=(100\times(TB_V - TB_H))/((TB_V+TB_H)) \qquad (1)$$

where, TB_V = brightness temperature measured at vertical polarization

TB_H = brightness temperature measured at horizontal polarization

TB is composed of the emissivity (ϵ) and the surface temperature (T_S) as shown in the following equation.

$$TB=\epsilon T_S \qquad (2)$$

Hence, the brightness temperatures in vertical (TB_V) and horizontal (TB_H) polarizations depend on the emissivity values of the surfaces as observed by the sensors in vertical (ϵ_V) and horizontal (ϵ_H) polarizations respectively.

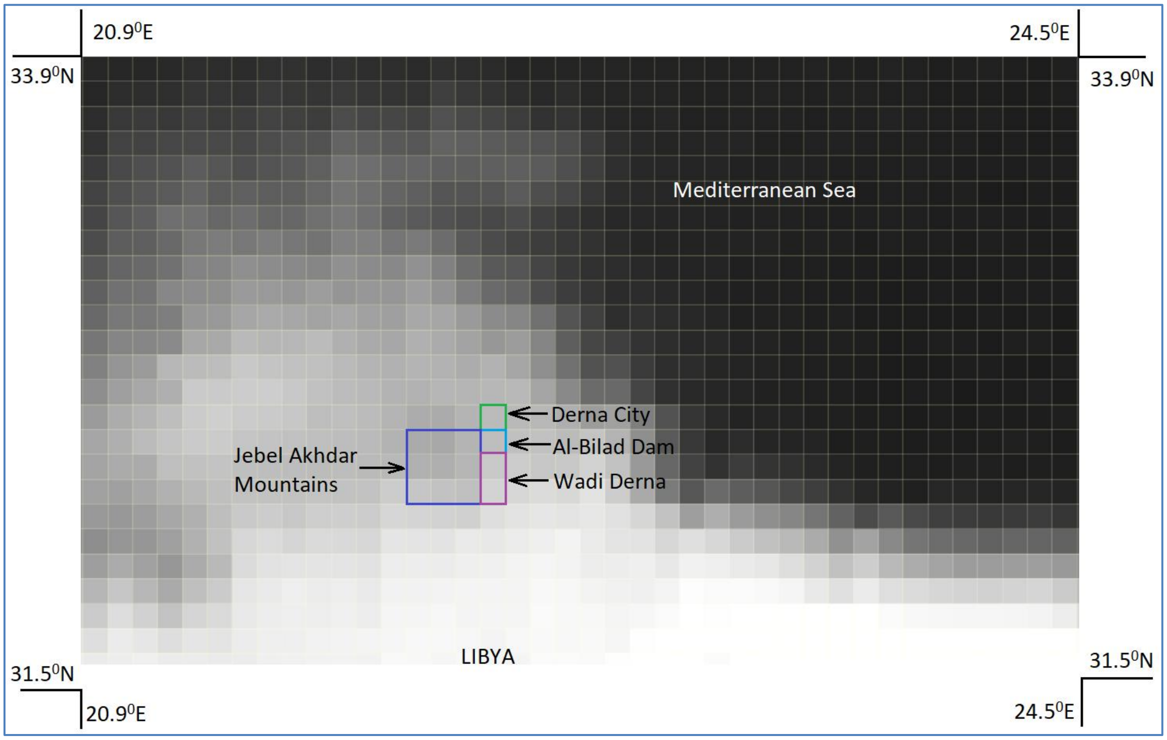

Fig. 2. AMSR-2 image of the study area showing Jabel Akhdar Mountains, Derna City, a portion of the Mediterranean Sea etc.

$$TB_V = \epsilon_V . T_S \quad (3)$$

$$TB_H = \epsilon_H . T_S \quad (4)$$

Equation (1) is thus used to eliminate surface temperature (T_S) values from the expression, so that the difference in emissivity alone can be determined as-

$$PI = (100 \times (\epsilon_V.T_S - \epsilon_H.T_S)) /((\epsilon_V.T_S + \epsilon_H.T_S))$$

$$= (100 \times (\epsilon_V - \epsilon_H))/((\epsilon_V + \epsilon_H)) \quad (5)$$

From equation (5) it is observed that the expression of PI is only dependent on the variations of the difference in emissivity values observed in vertical and horizontal polarizations. It is noteworthy that the emissivity in vertical polarization does not vary significantly with the variation in soil moisture or water content in the target object. However, in horizontal polarization it varies significantly. Hence, there will be a greater difference in emissivity value with the increase in soil moisture or water content in the target object. Thus, an increased PI value will necessarily indicate the increase in soil moisture content of the target area, possibly due to precipitation and water run-off. Another point mention worthy is the normalization factor 100, which is multiplied to the usual Polarization Index expression. This makes the values of the index vary in the range from -4 to +12, which is easy to read and analyse.

Hence, the daily PI variations are observed for possible indicative values, such as an abnormal rise in the value of PI on a particular day caused by the increase in soil moisture level, due to heavy precipitation. In case of any such abnormal rise, observed in just one area, similar conditions for other nearby areas are analysed. Abnormal rise in PI in several nearby locations is then correlated with actual flooding condition in nearby low-lying areas, such as the Derna city in this case.

The locations on the map which are observed in a typical passive microwave remote sensed brightness temperature image for extracting the brightness temperature values are shown in fig. 2. The fig. shows the locations of the Jebel Akhdar mountains, the Al-Bilad dam, the Wadi Derna River and the city of Derna beside the Mediterranean Sea. It is to be noted that the pixel size of the brightness temperature images used is 10 km × 10 km in resolution.

With a 10 km × 10 km resolution, passive microwave brightness temperature images cannot capture fine spatial details, as each pixel blends together all features within that large area. This blending often mixes signals from different surfaces—such as land, water, and vegetation—making it harder to interpret the data accurately. However, for larger area of study and regional level change detection, such a spatial resolution is

Fig. 3. Pre and Post flood variation of *PI* for Derna City in the month of September 2023

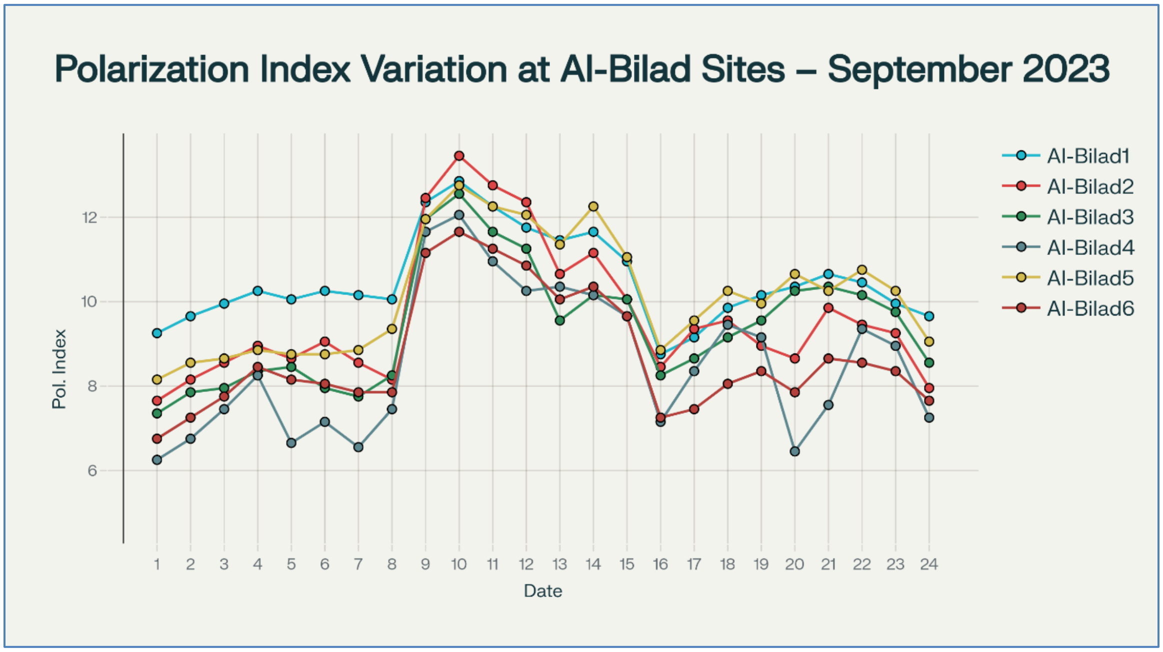

Fig. 4. Pre and Post flood variation of *PI* for the areas around Derna City in the month of September 2023

sufficient. The greatest advantage of such passive microwave remote sensing satellite data is the high temporal resolution. The satellite passes over the same place daily, with a global coverage. This advantage of high temporal resolution outperforms the disadvantage of low spatial resolution of such passive microwave sensor data.

Thus, the changes in PI values are observed from the passive microwave remote sensed brightness

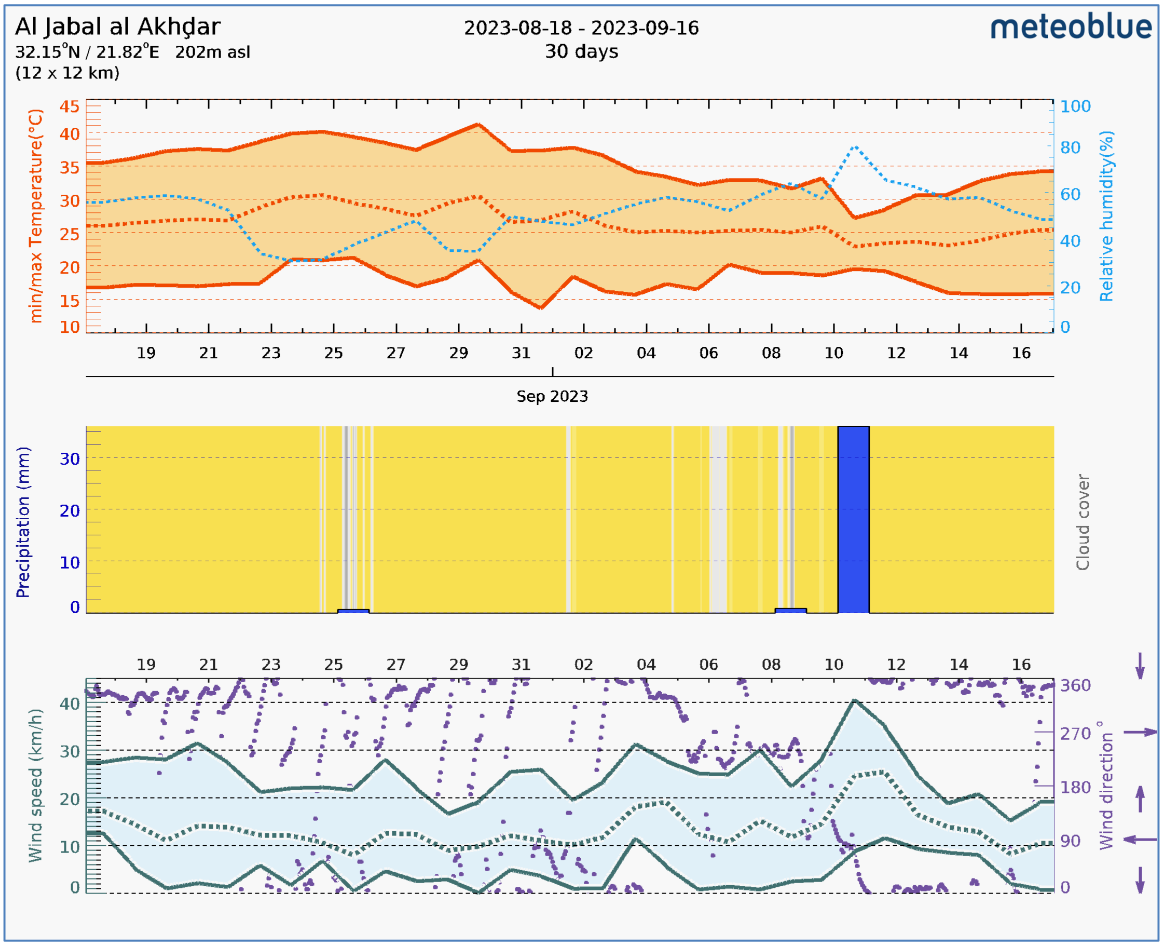

Fig. 5. Temperature, Precipitation and Wind Speed of Al-Akhdar area during 18 August - 16 September 2023

temperature data. The analysis of the variation of the PI values lead to the useful results in detecting the change in moisture content in soil, which is discussed in the following section.

3. Results and discussion

The Polarization Index (PI) values were studied for Derna city and its surrounding areas. These regions are known to have water run-off during heavy rainfall. The values were then plotted against the days of September 2023, as shown in Figs. 3 and 4.

A sharp increase in the PI values was recorded between 10th and 12th September. The values rose nearly 120% higher than the normal level. This unusual jump is most likely linked to the heavy rainfall and flooding that occurred on 11th September.

Interestingly, the rise in PI began even earlier. On the morning of 10th September, a steep increase was already visible in areas within and around Derna. These included the Jebel Akhdar Mountain Region, the Al-Bilad Dam, and the Wadi Derna River course. In Table 1, these areas are identified as Al-Bilad1 through Al-Bilad6. Since, the data considered from the satellite are from the day time passes of the satellite, the values considered for PI computations are the morning time (morning pass or descending node: ~01:30 AM local time) values of TB.

The Polarization Index (PI) values on the morning of 10th September showed a steep rise in areas near Derna. This sudden increase pointed to an abnormal pattern. These values were measured in regions that later contributed to the floodwaters flowing through Derna. The water followed the Wadi Derna river course after heavy rainfall in those areas from the morning of 10th September.

This intense rainfall caused a significant increase in soil moisture levels across the wide mountain region near

Derna. Such an increase is a clear sign of soil saturation, which usually happens under extreme precipitation. The saturated conditions eventually triggered a massive water flow through the Wadi Derna. This heavy surge inundated large portions of the city. The destruction was worsened by the collapse of the Al-Bilad Dam and the Abu Mansur Dam.

The exceptional rainfall over the Jebel Akhdar mountain region is also confirmed by the Meteoblue report [12], shown in fig. 5. The data highlights precipitation during 10–11 September that is far beyond ordinary levels. This evidence aligns with what was observed in the PI values. The extremely high rainfall recorded in the mountains during the early hours of 11th September supports the experimental finding of unusually high PI values on that day.

A comparison of figs. 3 and 4 with the actual precipitation and flooding in Derna reveals an important finding. The analysis shows that monitoring PI values in the Jebel Akhdar mountain region and along the Wadi Derna river course is crucial. A sudden rise in these values due to sharp increase in soil moisture caused by heavy rainfall, could serve as an early warning of possible flooding.

In reference to the present study, the figs. 3 and 4 show a significant spike in Polarization Index (PI) just before the flood event. The PI increase just one-day before the flood is approximately 70% from the baseline. Thus, tentatively the absolute value of PI threshold that could serve as an early flood alert trigger for the specific region is found to be 10. Clearly there is a one-day gap between the PI rise and the actual flooding, as observed from the results above, which demonstrates the potential of the method in flood prediction applications.

Thus, the continuous monitoring of the sudden soil moisture changes for such large areas can be done using passive microwave remote sensing. This approach could play a key role in predicting floods in the valleys, caused by heavy rainfall in nearby mountainous regions. Such a method is likely to reduce the impact of similar disasters in the future, by providing early warning signals.

4. Conclusions

Monitoring of soil moisture conditions of an area can be a useful exercise in predicting the occurrences of natural disasters such as flood. During the monsoon season, when the conventional optical remote sensing is not useful due to cloud cover, the microwave remote sensing can provide an opportunity to monitor the areas through continuous, near real-time observation. Thus, the city of Derna in Libya experiencing a devastating flood in September 2023, could have been alerted in advance, through the monitoring of its surrounding areas by passive microwave remote sensing. The paper presents the results of such a study done on the areas surrounding Derna where a high value of microwave polarization index, computed from satellite observations of one day before flood, is indicative of an impending heavy water run-off from the mountains to the low-lying areas of the city, causing the extensive deluge. The use of passive microwave remote sensing with high temporal resolution may thus help in identifying the potential occurrence of flood, by monitoring the abrupt increase in soil moisture, as described in the paper. This study may be extended further to other areas of the world having similar geographical conditions, for possible application of the method in predicting flood occurrences. While the approach demonstrates a significant potential, the 10 km × 10 km spatial resolution of passive microwave imagery imposes limitations. Particularly there are limitations in capturing fine-scale variations and avoiding mixed-pixel effects. Future research could test this approach in other flood-prone cities with similar landscapes. Using higher-resolution optical imagery alongside passive microwave data would help capture more detail on the ground. Ground-based measurements could also be added to check and refine the satellite results. Together, these steps would show how well the method works across different climates and types of terrain.

Acknowledgements

The authors would like to acknowledge the ADBU Centre for Geoinformatics, for providing the necessary facilities for experimental research on Microwave Remote Sensing applications.

Data Availability

The data used for the work is freely available on the Globe Portal System (G-Portal) of Japan Aerospace Exploration Agency (JAXA) at- https://gportal.jaxa.jp/gpr/

Funding

There was no funding support received from any agency for the work presented in the paper.

Authors' contributions

Bikramjit Goswami: Data Analysis and Manuscript writing *(email: bikramjit.goswami@dbuniversity.ac.in)*.
Manoranjan Kalita: Supervision of the work and Manuscript Upgradation *(email: director.sot@dbuniversity.ac.in)*.

Disclaimer: The contents and views expressed in this research article are the views of the authors and do not necessarily reflect the views of the organizations they belong to.

References

Abu-Aziza, E.B., El-Barasi, Y.M. and Rahil, R.O., 2017, "Flora, Vegetation and Human Activities of Wadi Der-na-El-Jabal", *ContROL*, 1, 6. https://doi.org/10.13140/RG.2.2.27645.26086

Bauer, P., 1995, "Passive microwave remote sensing of atmospheric parameters", In *1995 International Geoscience and Remote Sensing Symposium, IGARSS'95. Quantitative Remote Sensing for Science and Applications*, 2, 873-875, IEEE. https://doi.org/10.1109/IGARSS.1995.521083

Bindlish, R., Crow, W.T. and Jackson, T.J., 2004, "Potential role of passive microwave remote sensing in improving flood forecasts", In *IGARSS 2004. 2004 IEEE International Geoscience and Remote Sensing Symposium*, 3, 1866-1869. https://doi.org/%2010.1109/IGARSS.2004.1370703.

Febrian, R.D., Kim, W., Lee, Y., Kim, J. and Choi, M., 2025, "Estimation of Flood Inundation Area Using Soil Moisture Active Passive Fractional Water Data with an LSTM Model", *Sensors*, 25, 8, 2503, https://doi.org/10.3390/s25082503

Hajji, S. et al., 2025, "Enhancing flood prediction through remote sensing, machine learning, and Google Earth Engine", *Frontiers in Water*, 7, https://doi.org/10.3389/frwa.2025.1514047

Hariharan, T.A. and Pandey, P.C., 1983, "Passive microwave remote sensing of the atmosphere and ocean", *Proceedings of the Indian Academy of Sciences Section C: Engineering Sciences*, 6, 233-254. https://doi.org/10.1007/BF02842886

Kasim, A.A. et al., 2025, "Remote sensing of root zone soil moisture: A review of methods and products", *Journal of Hydrology*, 656, 133002, https://doi.org/10.1016/j.jhydrol.2025.133002

Marshall, M., 2023, "Libya floods: how climate change intensified the death and devastation", *Nature*, 621, 7979, 452-453, https://doi.org/10.1038/d41586-023-02899-6

Meteoblue, 2024, "Weather Archive Al Jabal Al Akhdar", available at https://www.meteoblue.com/en/weather/historyclimate/weatherarchive/al-jabal-al-akhdar (Accessed 16 January 2024).

Mokkenstorm, L.C., van den Homberg, M.J.C., Winsemius, H. and Persson, A., 2021, "River Flood Detection Using Passive Microwave Remote Sensing in a Data-Scarce Environment: A Case Study for Two River Basins in Malawi", *Frontiers in Earth Science*, 9, https://doi.org/10.3389/feart.2021.670997

Njoku, E.G., 1982, "Passive microwave remote sensing of the earth from space—A review", *Proceedings of the IEEE*, 70, 7, 728-750. https://doi.org/10.1109/PROC.1982.12380

Njoku, E.G. and Entekhabi, D., 1996, "Passive microwave remote sensing of soil moisture", *Journal of Hydrology*, 184, 1-2, 101-129. https://doi.org/10.1016/0022-1694(95)02970-2

Pampaloni, P., 2014, "Looking at the earth as a planet: Passive microwave remote sensing of land surfaces", *URSI Radio Science Bulletin,* 2014, 351, 5-28. https://doi.org/10.23919/URSIRSB.2014.7909842

Peichl, M., Dill, S., Jirousek, M. and Suess, H., 2007, "Passive microwave remote sensing for security applications", *In 2007 European Radar Conference*, 32-35. https://doi.org/10.1109/EURAD.2007.4404929

Peichl, M., Dill, S., Jirousek, M. and Schreiber, E., 2015, "On the use of passive microwave remote sensing by airborne platforms", *In 2015 16th International Radar Symposium (IRS)*, 225-230. https://doi.org/10.1109/IRS.2015.7226382

Ulaby, F., 1976, "Passive microwave remote sensing of the Earth's surface", *IEEE Transactions on Antennas and Propagation*, 24, 1, 112-115. https://doi.org/10.1109/TAP.1976.1141299.